Broadband Gap-Coupled Variations of Modified Equilateral Triangular Microstrip Antennas

Amit A. Deshmukh

Professor and Head, EXTC Dept.

DJ Sanghvi College of Engineering

Vile Parle (W) Mumbai, India

S. B. Nagarbowdi, N. V. Phatak,

K. A. Lele, S. A. Shaikh, A. A. Desai,

S. Agrawal

PG student, EXTC Dept.

D. J. Sanghvi College of Engineering

Vile Parle (W) Mumbai, India

ABSTRACT

The compact variations of equilateral triangular microstrip antenna are realized by placing the shorting post along the zero field line at its fundamental TM_{10} mode. In this paper various proximity fed broadband configurations of complementary of shorted 60^0 Sectoral microstrip antennas are proposed. The complementary of shorted 60^0 Sectoral patch yields bandwidth of more than 370 MHz (>40%). To increase the bandwidth of complementary shorted 60^0 Sectoral antenna, its gap-coupled configuration by splitting the patch into two unequal dimension shorted patches is proposed, which gives bandwidth of nearly 500 MHz (~43%). Further increase in the gain and BW of shorted complementary Sectoral patch is obtained by gap-coupled it with another Shorted 600 Sectoral microstrip antenna. This gap-coupled configuration yields bandwidth of around 550 MHz (>55%). Further increase in bandwidth of gap-coupled configuration is realized by cutting the slot on the edge of complementary shorted patch. The gap-coupled slot cut configuration gives bandwidth of around 570 MHz (~8%). Due to shorted patch shorted gap-coupled antennas shows higher cross polar radiation pattern with a peak gain of nearly 5 dBi.

Keyword

Equilateral triangular microstrip antenna, Compact microstrip antenna, Shorted 60^0 Sectoral microstrip antenna, Complementary of Shorted 60^0 Sectoral microstrip antenna Gap-coupled, Rectangular slot, Proximity feed

1. INTRODUCTION

By suspending the radiating patch above the ground plane (i.e. by using air substrate), broadband microstrip antenna (MSA) has been realized [1 – 3]. The thicker substrate with unity dielectric constant (air) reduces the quality factor of the cavity below the patch to realize broader bandwidth (BW). To realize the input impedance matching on thicker substrates (h > 0.06 to $0.08\lambda_0$), proximity feeding techniques has been used [4, 5]. In proximity feeding technique, capacitance formed between coupling strip and the radiating patch compensates for the probe inductance due to thicker substrate that yields input impedance matching. The compact MSAs are realized by shorting the patch along the zero field line at fundamental patch mode and further by using half of the patch size [1 – 3, 6]. The BW of compact shorted MSAs has been increased by using their gap-coupled and stacked configurations. The

compact variation of equilateral triangular MSA (ETMSA) is realized by placing the shorting plate/post along the zero field line of fundamental TM_{10} mode, and it realizes compact shorted 60^0 and complementary of shorted 60^0 Sectoral MSAs [1]. The BW of shorted 60^0 Sectoral MSA has been increased by using thicker air substrate in conjunction with proximity feeding technique [7]. It yields BW of more than 450 MHz (> 40%). In this paper, broadband proximity fed gap-coupled variations of complementary of shorted 60^0 Sectoral MSA is proposed. The proximity fed configuration of complementary of shorted 60^0 Sectoral MSA (C-60^0 S-MSA) yields BW of more than 370 MHz (>40%). To further increase its BW, complementary configuration is divided into two unequal shorted patches. This gap-coupled configuration yields BW of nearly 500 MHz (~43%). Due to shorted patch, radiation pattern in complementary and its gap-coupled variation shows higher cross-polar levels with gain of around 3 dBi over most of the BW. To increase the gain and BW of C-60^0 S-MSA, its gap-coupled configuration with shorted 60^0 Sectoral MSA is proposed. It yields BW of nearly 550 MHz (>55%) with gain of above 3 dBi over most of the BW. Further increase in BW of above gap-coupled configuration is realized by cutting the slot inside the complementary shorted MSA. The slot in shorted patch does not introduce any new resonant mode but reduces the frequency of higher order $TM_{1/4,1}$ mode of the shorted patch and along with fundamental shorted $TM_{1/4,0}$ mode yields BW of more than 570 MHz (~58%). This slot cut gap-coupled configuration shows similar radiation pattern and gain characteristics to that shown in above gap-coupled configuration. All these shorted MSAs were first analyzed using IE3D software on finite square ground plane of side length 30 cm [8]. Further in measurements patches were fabricated using copper plate having finite thickness and were supported in air using foam spacers. The foam spacers have dielectric constant of nearly unity hence it does not affect the overall dielectric constant of the substrate. The antennas were fed using N-type connector of 0.32 cm inner wire diameter. The impedance measurement was carried out using ZVH – 8 vector network analyzer whereas antenna pattern and gain were measured in lab wherein minimum reflection from surrounding object was ensured. The RF source (SMB – 100A) and spectrum analyzer (FSC – 6) were used in gain and pattern measurement. Due to shorted patches proposed antenna shows higher cross polar radiation pattern hence gives elliptical polarization over complete BW. Therefore proposed configuration can find applications in multi-path propagation

environment wherein antennas with higher cross polar levels will lead to lesser signal loss.

2. PROXIMITY FED SHORTED COMPACT VARIATIONS OF ETMSAs

The proximity fed ETMSA is shown in Fig. 1(a, b). The units of the dimension and frequencies shown in all the figures and their captions are in cm and MHz, respectively. The proposed configurations are designed to cover 700 to 1300 MHz frequency range. Therefore ETMSA side length (S) is calculated such that its TM_{10} mode frequency is around 1000 MHz. To realize larger BW, ETMSA is designed on air substrate of thickness 'h' = 3.0 cm (h ~ $0.1\lambda_0$). Using the resonance frequency equation of ETMSA as given in equation (1), 'S' is calculated [2]. While calculating the frequency, the effective patch side length (S_e) needs to be considered. The effective length accounts for extension in length due to fringing fields present towards the open circuit edges of the patch side length. While using thinner substrates (h < $0.03\lambda_0$) 'S_e' is calculated by using equation (2) [2]. However equation (2) does not give accurate results for h > $0.03\lambda_0$. Further closed form equations for fringing field extension length are not directly available for thicker substrate. Hence patch side length cannot be accurately calculated for thicker substrate at different resonant frequencies.

$$f_{TMmn} = \frac{2c\sqrt{m^2 + mn + n^2}}{3S_e\sqrt{\varepsilon_{re}}} \qquad (1)$$

$$S_e = S + \frac{4h}{\sqrt{\varepsilon_{re}}} \qquad (2)$$

where, c = velocity of light = 3×10^8 (m/s),
S_e = effective patch side length,
m and n = mode indices

h = substrate thickness
ε_{re} = effective dielectric constant

In ETMSA, an artificial neural network model to calculate patch side length and edge extension length in terms of substrate thickness for substrate thickness varying from 0.04 to $0.1\lambda_0$ and for frequencies increasing from 700 to 6000 MHz is reported [9]. Using the same patch side length that gives f_{TM10} around 1000 MHz is calculated. It is found to be 13.8 cm. The proximity feed ETMSA is simulated for h = 3.0 and h1 = 2.8 cm and their resonance curve plots are shown in Fig. 1(d). The plots shows two peaks and surface current distribution at them are shown in Fig. 2(a, b). In ETMSA, field variations are symmetrical with respect to patch centroid point. At TM_{10} mode field/surface current shows one half wavelength variations along patch side length and along its height, with zero field at the centroid point [2]. The next mode in ETMSA is TM_{11} [2]. Depending upon the feed position, at TM_{11} mode, field shows one half wave length variations from the centroid point and towards the patch vertex [2]. The next higher order mode is TM_{20}, at which field shows two half wavelength variations along the side length and along height of the patch [2]. At TM_{10} mode, compact variation of ETMSA, a complementary of shorted 60^0 Sectoral MSA (C-60^0 S-MSA) is derived by placing the shorting plate along the zero field line and by using larger section of the shorted patch,

as shown in the Fig. 1(c). The C-60 S-MSA is simulated and its resonance curve plot for xf = 2.0 and yf = 0.0 cm is shown in Fig. 1(d). The plot shows two peaks and surface current distribution at them is shown in Fig. 2(c, d). The dominant mode in C-60^0 S-MSA is shorted TM_{10} at which surface current shows quarter wavelength variation along shorted length.
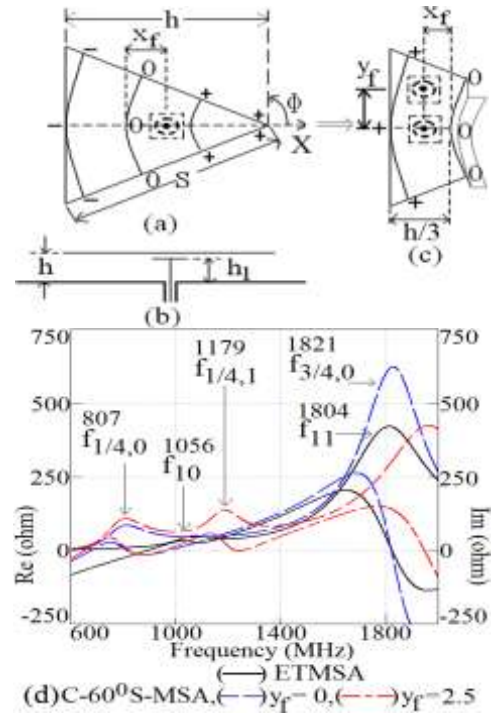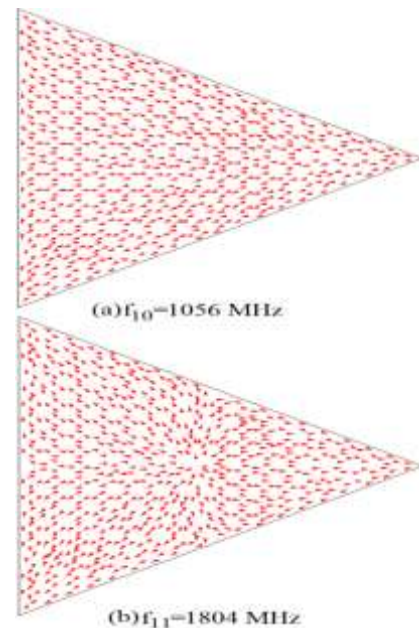

Fig 1: (a) Top and (b) side views of proximity fed ETMSA, (c) C-60^0 S-MSA, and their (d, e) resonance curve plots

(a)f_{10}=1056 MHz

(b)f_{11}=1804 MHz

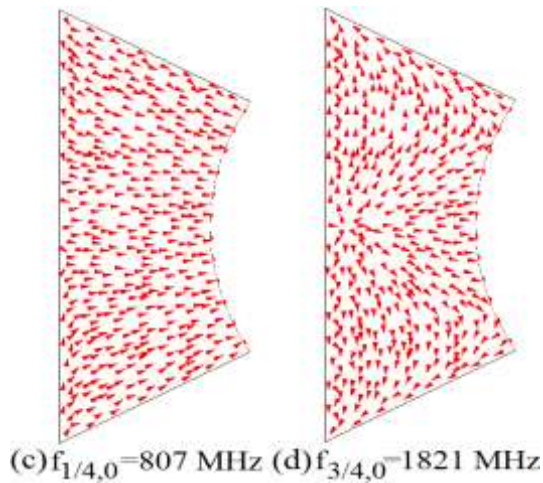(c) $f_{1/4,0}$=807 MHz (d) $f_{3/4,0}$=1821 MHz

Fig 2: Surface current distributions for proximity fed (a, b) ETMSA and (c, d) C-60^0 S-MSA at first two resonant modes

This mode is also referred to as $TM_{1/4,0}$ mode. Here the first index corresponds to odd integer multiples of quarter wavelength variation along shorted length (mixed boundary condition) and the second index refers to integer multiples of half wavelength variations along the orthogonal shorted patch dimension (identical boundary condition). The shorted TM_{20} ($TM_{3/4,0}$) mode is also present in C-60^0 S-MSA as it also shows zero fields near the centroid point. At shorted TM_{20} ($TM_{3/4,0}$) mode currents shows quarter wavelength variation along shorted length. The resonance curve plot for C-60^0 S-MSA for offset proximity feed point location, i.e. x_f = 2.0 and y_f = 2.5 cm is shown in Fig. 1(d). It shows excitation of new mode near the frequency of 1179 MHz. The surface current distribution at this new mode is shown in Fig. 3.
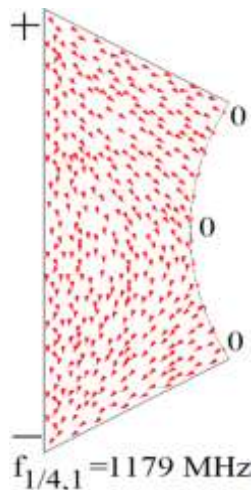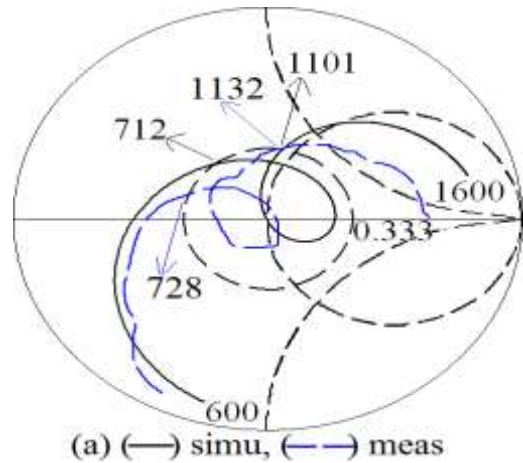

$f_{1/4,1}$=1179 MHz

Fig 3: Surface current distributions at $TM_{1/4,1}$ mode for proximity fed C-60^0 S-MSA

The current shows one quarter wavelength variation along shorted patch length and one half wavelength variation along shorted patch width. Due to this variation this mode I referred to as $TM_{1/4,1}$ mode. The surface currents at $TM_{1/4,0}$ mode are directed along horizontal direction due to which radiation

pattern at the same mode shows E-plane directed along $\Phi = 0^0$. At $TM_{1/4,1}$ mode maximum contribution of currents are directed along vertical direction hence E-plane is aligned along $\Phi = 90^0$. Similar to the proximity fed compact configuration reported in [7] the broadband response at $TM_{1/4,0}$ mode in C-60^0 SMSA is obtained by carrying out parametric study on strip dimension and its position below the patch and the substrate thickness for the same. The optimized input impedance plot is shown in Fig. 4(a). The simulated BW is 389 MHz (42.9%). The patch was fabricated on finite ground plane using copper plate. The same was supported in air using foam spacer support placed towards the antenna corners. The measurement was carried out using ZVH-8 Vector network analyzer. The measured BW is 404 MHz (43.4%) as shown in Fig. 4(a). The fabricated prototype of the configuration is shown in Fig. 4(b). The radiation pattern at center frequency of BW in the bore sight direction and gain variation over the BW are shown in Fig. 5(a, b). Due to the shorted patch the pattern shows higher cross polar levels. The E and H-planes are aligned along $\Phi = 0^0$ and 90^0, respectively. Also due to shorted patch antenna gain is above 3 dBi over complete BW. To further increase the BW the gap-coupled configuration of shorted C-60^0 S-MSA is studied as shown in Fig. 5(c).
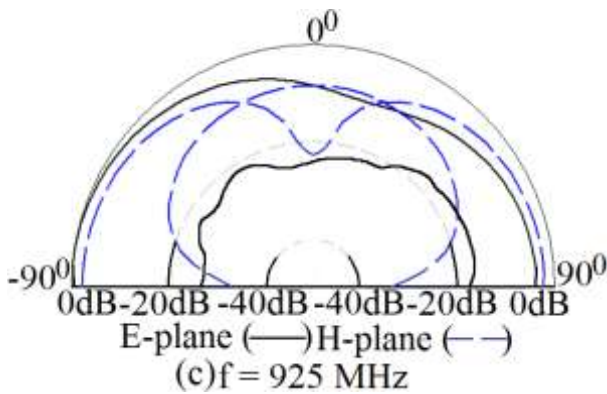

(a) (——) simu, (— —) meas

(b)

Fig 4: (a) Input impedance plots, (b) fabricated prototype and (c) radiation pattern at center frequency of BW for proximity fed C-60^0 S-MSA

The shorted patch is divided along its width with unequal lengths of two shorted patches. The proximity feed is placed below the patch and it is placed symmetric with respect to two patches. The realized BW depends upon the difference in the resonance frequencies of two shorted patches. The optimum BW is obtained for $l_1 = 2.4$ and $l_2 = 3.2$ cm, as shown in Fig. 5(b). The simulated BW is 496 MHz (43.1%) whereas the measured BW is 502 MHz (42.9%) as shown in Fig. 5(c).
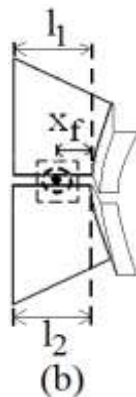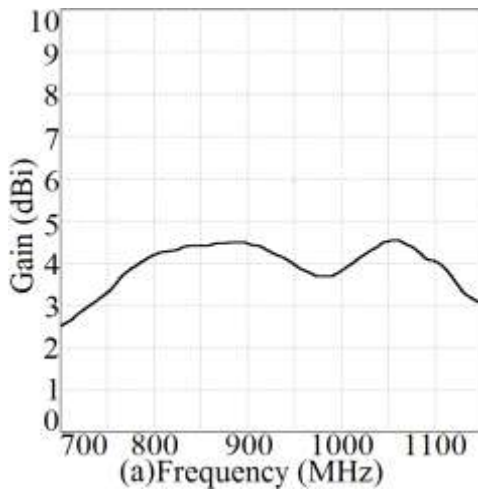

Fig 5: (a) Gain variation over BW for proximity fed C-60^0 S-MSA, (b) proximity fed gap-coupled C-60^0 S-MSAs and its (c) input impedance plots

This gap-coupled configuration yields nearly the same gain and radiation pattern characteristics to that given by the MSA shown in Fig. 1(c). The gap-coupled configuration of shorted 60^0 Sectoral MSA along with its complementary configuration is shown in Fig. 6(a). The broadband response is realized by optimizing the spacing between two shorted MSAs as well as the radius of shorted 60^0 Sectoral MSA. For h = 4.0, r = 6.8 and g = 0.2 cm, broadband response as shown in Fig. 6(b) is obtained.
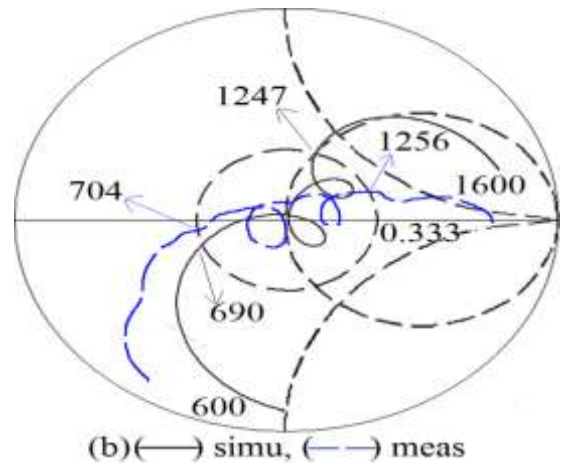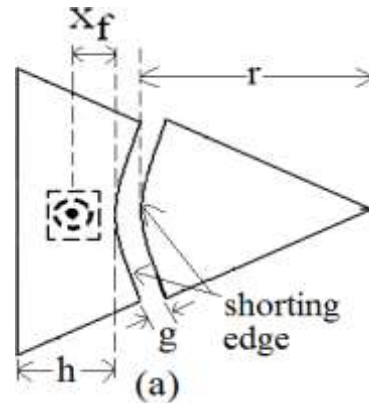

Fig 6: (a) Proximity fed C-60^0 S-MSA gap-coupled to shorted 60^0 Sectoral MSA and its (b) input impedance plots

The simulated BW is 557 MHz (57.5%) whereas the measured BW is 552 MHz (56.3%). The radiation pattern in the bore sight direction at center frequency of operating BW and gain variation over BW is shown in Fig. 7(a, b). The E and H-planes are aligned along $\Phi = 0^0$ and 90^0, respectively. Due to shorted patch, higher cross polar levels are observed in the radiation pattern plot. The antenna gain is more than 3 dBi over the complete BW. Further increase in the BW of above gap-coupled configuration is obtained by cutting the rectangular slot on the edge of C-60^0 S-MSA as shown in Fig. 7(c). The resonance curve plots for shorted configuration shown in Fig. 6(a) and slot cut configuration shown in Fig. 7(c) is shown in Fig. 8(a).
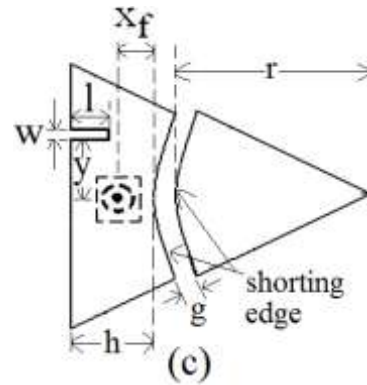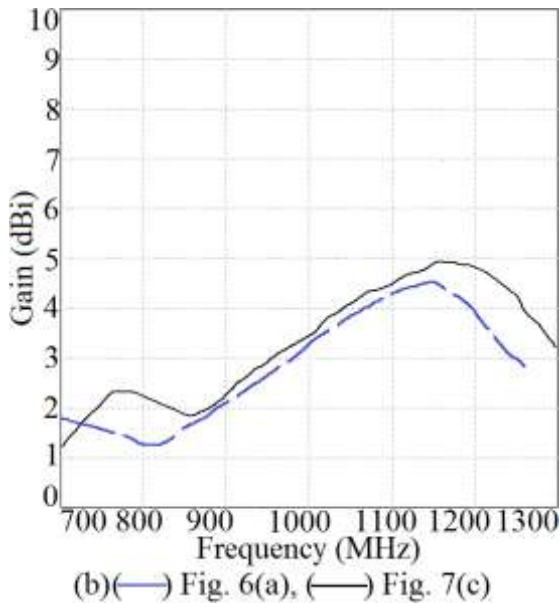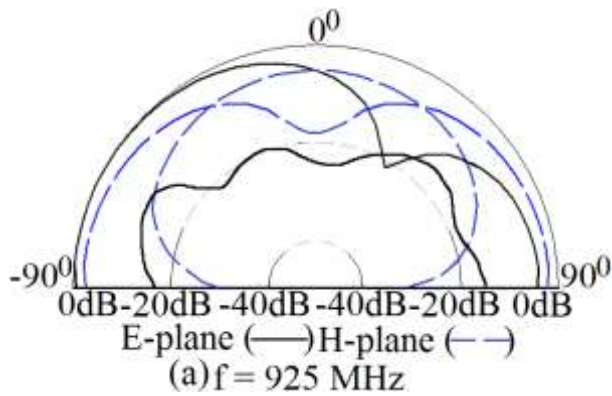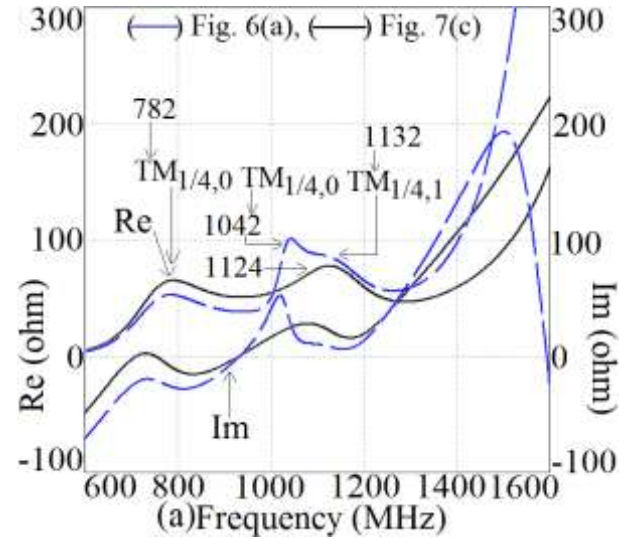

(a) f = 925 MHz

(b)(——) Fig. 6(a), (——) Fig. 7(c)

Fig 7: (a) Radiation pattern and (b) gain variation over the BW for proximity fed C-60^0 S-MSA gap-coupled to shorted 60^0 Sectoral MSA, and (c) proximity fed slot cut C-60^0 S-MSA gap-coupled to shorted 60^0 Sectoral MSA

The slot tunes between $TM_{1/4,1}$ mode frequency on shorted C-60^0 S-MSA with respect to $TM_{1/4,0}$ mode frequencies on the respective shorted patches to realize increase in the overall BW. For y = 2.5, w = 0.8, l = 4.0 cm, the optimum input impedance plots are shown in Fig. 8(b). The simulated BW is 575 MHz (57.6%). The experiment was carried out by fabricating the patch using copper plate supported by foam spacers above the ground plane. The measured BW is 576 MHz (58.6%). The radiation pattern at center frequency and gain variation over the BW are shown in Figs. 8(c) and 7(b), respectively.
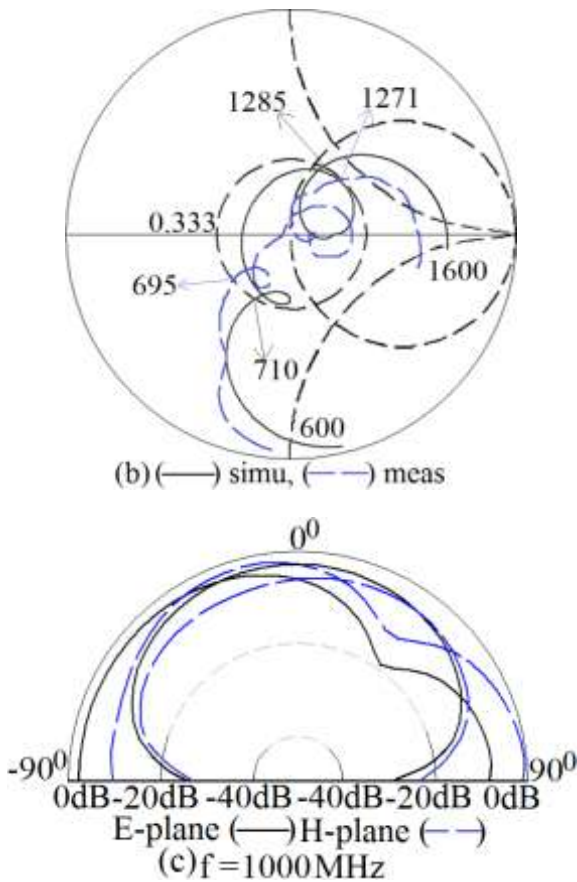

(a)Frequency (MHz)

Fig 8: (a) Resonance curve plots for two shorted MSAs, (b) input impedance plots for proximity fed slot cut C-60^0 S-MSA gap-coupled to shorted 60^0 Sectoral MSA, and its (c) radiation pattern at center frequency of the BW

The pattern shows higher cross polar levels due to vertical surface current components at modified TM$_{1/4,1}$ mode in proximity fed slot cut C-60^0 S-MSA. The results for all the shorted variations of C-60^0 S-MSA are tabulated in Table 1. In terms of operating BW and gain gap-coupled configuration of C-60^0 S-MSA with shorted 60^0 Sectoral MSAs yields optimum result.

Table 1 – Comparison between variations of C-60^0 S-MSA

Configuration shown in Fig.	Simulated BW MHz %	Measured BW MHz, %
1(c)	389, 42.9	404, 43.4
5(b)	496, 43.1	502, 42.9
6(a)	557, 57.5	552, 56.3
7(c)	575, 57.6	576, 58.6

3. CONCLUSIONS

The broadband proximity fed variations of compact C-600 S-MSAs are proposed. Amongst all the proposed configurations, gap-coupled configuration of C-60^0 S-MSA with shorted 60^0 Sectoral MSA yields optimum response in terms of BW and gain. Although the proposed configurations shows radiation pattern with higher cross polar levels, but they will be useful in applications wherein multipath propagation effect, affects the polarization purity of the received signal.

4. REFERENCES

[1] Garg, R., Bhartia, P., Bahl, I., Ittipiboon, A., 2001. Microstrip Antenna Design Handbook, Artech House, USA.

[2] Kumar, G., Ray, K. P., 2003. Broadband Microstrip Antennas, 1st edn., Artech House, USA.

[3] B. Bhartia and I. J. Bahl, Microstrip Antennas, USA, 1980.

[4] Wong, K. L., 2002. Compact and Broadband Microstrip Antennas, 1st edn., John Wiley & sons, Inc., New York, USA.

[5] Cock, R. T., and Christodoulou, C. G., Design of a two layer capacitively coupled, microstrip patch antenna element for broadband applications, IEEE Antennas Propag. Soc. Int. Symp. Dig., vol. 2, 1987, pp. 936-939.

[6] Deshmukh, Amit A., and Kumar, G., Compact Broadband gap-coupled Shorted L-shaped Microstrip Antennas, Microwave and Optical Technology Letters, vol. 47, no. 6, 20th Dec. 2005, pp. 599 – 605.

[7] Deshmukh, Amit A., et. al., "Broadband Gap-coupled Shorted 60° Sectoral Microstrip Antenna", Proceedings of ICCT-2015, 25th and 26th September 2015, Mumbai, India, (http://www.ijcaonline.org/proceedings/icct2015/number 5/22662-1563)

[8] IE3D 12.1, Zeland Software, Freemont, USA, 2004.

[9] Deshmukh, Amit A., Venkata, A. P. C., Kulkarni, S. D., and Nagarbowdi, S., Artificial Neural Network Model for Suspended Equilateral Triangular Microstrip Antennas, Proceedings of ICCICT - 2015, 15th - 17th January 2015, Mumbai, India